haematologica
Journal of the Ferrata Storti Foundation

Novel tripartite *CPSF7::RARG::CPSF7* fusion confers primary ATRA resistance in atypical acute promyelocytic leukemia

by Xiaosu Zhou, Zhanglin Zhang, Fang Xu, Mei Jiang, Yang Zhang, Panxiang Cao, Jiancheng Fang, Xiaoli Ma, Fang Wang, Jiaqi Chen, Xue Chen, Ping Wu, Tong Wang, Yue Lu and Hongxing Liu

Received: March 15, 2026.
Accepted: May 18, 2026.

Citation: Xiaosu Zhou, Zhanglin Zhang, Fang Xu, Mei Jiang, Yang Zhang, Panxiang Cao, Jiancheng Fang, Xiaoli Ma, Fang Wang, Jiaqi Chen, Xue Chen, Ping Wu, Tong Wang, Yue Lu and Hongxing Liu. Novel tripartite CPSF7::RARG::CPSF7 fusion confers primary ATRA resistance in atypical acute promyelocytic leukemia.
Haematologica. 2026 May 28. doi: 10.3324/haematol.2026.300904 [Epub ahead of print]

Novel tripartite *CPSF7*::*RARG*::*CPSF7* fusion confers primary ATRA resistance in atypical acute promyelocytic leukemia

Xiaosu Zhou[1*], Zhanglin Zhang[2*], Fang Xu[3*], Mei Jiang[4], Yang Zhang[1,5], Panxiang Cao[5], Jiancheng Fang[5], Xiaoli Ma[5], Fang Wang[5], Jiaqi Chen[1,5], Xue Chen[1,5], Ping Wu[5], Tong Wang[5], Yue Lu[3#], Hongxing Liu[1,5,6#]

[1]Precision Medicine Center, Beijing Lu Daopei Institute of Hematology, Beijing, China;

[2]Department of Blood Transfusion, The First Affiliated Hospital of Nanchang University, Nanchang, China;

[3]Department of Transplantation, Hebei Yanda Lu Daopei Hospital, Langfang, China;

[4]Department of Clinical Laboratory, the First Affiliated Hospital, Jiangxi Medical College, Nanchang University, Nanchang, China;

[5]Division of Pathology & Laboratory Medicine, Hebei Yanda Lu Daopei Hospital, Langfang, China;

[6]Division of Pathology & Laboratory Medicine, Beijing Lu Daopei Hospital, Beijing, China;

*Xiaosu Zhou, Zhanglin Zhang, and Fang Xu contributed equally to this study.

Correspondence

Hongxing Liu, Precision Medicine Center, Beijing Lu Daopei Institute of Hematology, Beijing, China, 100176. Email: starliu@pku.edu.cn.

Yue Lu, Department of Transplantation, Hebei Yanda Lu Daopei Hospital, Langfang, China, 065201. Email: dpluyue@sina.com.

Running Title: Tripartite *CPSF7*::*RARG*::*CPSF7* fusion in aAPL

Keywords

acute promyelocytic leukemia, gene fusion, RARG, CPSF7, truncation mutation

Fundings

This work was supported by the Natural Science Foundation of China (82570228) and the Hebei Provincial Medical Science Research Project (20261157).

Data-sharing statement

For original data, please contact starliu@pku.edu.cn on reasonable request.

Disclosures

The authors declare no conflicts of interest.

Contributions

HL, ZZ and XZ designed the experiments, supervised the study and analysis, and wrote the manuscript; FX and YL collected clinical data; MJ, YZ, XM, FW, JC, XC, PW and TW performed and analyzed the experiments; PC and JF analyzed the bioinformation data. All authors discussed the results and implications of the manuscript.

Acknowledgments

The authors thank Siyuan Liu for his help in bioinformatic analysis and valuable discussions.

Supplementary data

Supplementary material can be found online in the Supporting Information section at the end of this article.

To the Editor:

Acute promyelocytic leukemia (APL) is a distinct subtype of acute myeloid leukemia (AML) characterized by pathognomonic morphological features and a rapidly progressive, fatal natural course. Classical APL, defined by the *PML*::*RARA* fusion gene, has achieved excellent outcomes with all-trans retinoic acid (ATRA) and arsenic trioxide (ATO) treatment. In contrast, a small subset of patients presents with an APL phenotype driven by individually rare and diverse retinoic acid receptor (*RAR*) rearrangements involving *RARA*, *RARB*, and *RARG* [1-7]. These cases have been previously described as "APL-like AML with non-*PML*::*RARA* (atypical) translocations", we will refer to this entity as "atypical APL (aAPL)" given their shared *RAR*-related biology.

To date, eight 5′ fusion partners for *RARG* have been identified, with *CPSF6* being the most frequent (16 reported cases) [5-13]. Notably, recent evidence suggests that all *RARG* fusions may exist as previously overlooked tripartite fusions (*X*::*RARG*::*X*/*Y*) rather than conventional bipartite fusions (*X*::*RARG*) [5,13]. In these cases, *RARG* 3′ splicing-mediated truncation of the ligand-binding domain (LBD) confers complete resistance to ATRA. Here, we report the first case of a novel tripartite *CPSF7*::*RARG*::*CPSF7* fusion, expanding the known spectrum of *RAR* fusion partners and reinforcing the paradigm of tripartite structures in *RARG* fusion positive aAPL (*RARG*-aAPL). This study was approved by the Ethics Committee of Hebei Yanda Lu Daopei Hospital.

A 42-year-old male was admitted with a one-month history of gingival bleeding, cutaneous ecchymosis, and significant weight loss. Initial laboratory evaluation revealed leukocytosis (white blood cells 45.7 × 10^9/L), anemia (hemoglobin 65.0 g/L), and thrombocytopenia (platelets 91.0 × 10^9/L). Coagulation profiles showed a prolonged prothrombin time (PT) of 15.0 s (reference, 9.4–12.5 s), a normal activated partial thromboplastin time (APTT) of 29.4 s (25.1–36.5 s), a decreased fibrinogen level of 1.6 g/L (2.0–4.0 g/L), and a markedly elevated D-dimer level of 16.2 mg/L (0–0.2 mg/L), consistent with coagulopathy and disseminated intravascular coagulation. Peripheral blood and bone marrow (BM) smears showed hypercellularity with abnormal promyelocytes (72% and 91.5%, respectively) characterized by coarse granules (Figure 1A) and intense myeloperoxidase (MPO) positivity (Figure 1B),

morphologically suggestive of classical APL. Flow cytometric analysis identified an abnormal promyelocytic population (90.3% of nucleated cells) that was positive for CD13, CD33, CD64, CD123, and MPO, with partial expression of CD56 and CD117, but negative for CD3, CD7, CD11b, CD14, CD34, CD38, and HLA-DR. Cytogenetic analysis showed a normal karyotype, and screening for *PML*::*RARA* (via fluorescence in situ hybridization and reverse transcription PCR) and 35 other common leukemia fusion genes (full panel in the Supplementary Table S1) was negative.

Initial treatment with ATRA and hydroxyurea was promptly initiated but failed to achieve cytoreduction (Figure 1C). Upon transfer to our center, the patient exhibited worsening hematological parameters and progressive coagulopathy, with a PT of 15.4 s, an APTT of 29.5 s, a further decrease in fibrinogen of 1.2 g/L, and a further elevation of D-dimer level to 37.8 mg/L. Subsequent regimens, including an idarubicin and cytarabine-based 3+7 regimen combined with venetoclax, as well as azacitidine/Lisaftoclax/ATRA, failed to control the disease (Figure 1C). BM morphology and immunophenotyping confirmed persistent disease, with abnormal promyelocytes accounting for 78.0% and 82.1% of nucleated cells, respectively.

Whole-transcriptome sequencing of the diagnostic BM sample demonstrated a gene-expression profile that clustered closely with a consecutive cohort of canonical *PML*::*RARA*-APL cases [14], while remaining significantly distinct from other AML subtypes and healthy controls (Figure 2A). Mutational analysis identified a somatic *ARID2* c.3563G>A/p.S1188N mutation with a variant allele frequency of 72.4 % (Figure 2B). Fusion gene analysis identified a tripartite *CPSF7* (exon 1_7)::*RARG* (exon 4_9)::*CPSF7* (exon 10@c.*1143) fusion (Figure 2C, Supplementary Figure S1A and S1B). Whole-genome sequencing confirmed the genomic breakpoints between *CPSF7* intron 7 and *RARG* intron 3 (Supplementary Figure S1C), and between *RARG* intron 9 and *CPSF7* exon 10 (Supplementary Figure S1D).

The treatment was modified to a combination of homoharringtonine (HHT), chidamide, selinexor, and gemtuzumab ozogamicin (GO). Following 10 days of therapy, BM promyelocytes decreased to 2.5%, and the patient achieved complete remission (CR) by day 24. He subsequently underwent haploidentical allogeneic hematopoietic stem cell transplantation (allo-HSCT) with his daughter as donor and remains in CR at 3-month follow-

up (Figure 1C).

Unlike previously reported tripartite *RARG* fusions that splice in-frame with 3′ coding sequences or transposons [5,13], this case involves the 3′ untranslated region (UTR) of *CPSF7*. Genomic rearrangement generated a de novo branch site (A) and splice acceptor (AG) within *CPSF7* exon 10, utilizing its polyadenylation signal (Figure 3A). This fusion truncates the *RARG*-LBD helices 11_12 (H11_12), a region essential for ligand-induced activation (Figure 3B), and introduces a novel C-terminal tail derived from the 3′ UTR. These findings define a previously uncharacterized mechanism of *RARG* 3′ fusion.

Cellular reporter assays confirmed that while a simulated bipartite CPSF7::RARG retained dose-dependent ATRA responsiveness (consistent with the wild-type RARG baseline), the patient-specific tripartite CPSF7::RARG::CPSF7 and the CPSF7::RARG-H11_12del mutant were entirely unresponsive to ATRA (Figure 3C). Notably, although the histone deacetylase 3 inhibitor (HDAC3i) chidamide markedly enhanced ATRA sensitivity in the bipartite CPSF7::RARG model—mirroring its effect on wild-type RARG—it completely failed to rescue transcriptional activity in the tripartite fusion and the H11_12del mutant models.

CPSF6 and its paralog CPSF7 are core subunits of the cleavage factor Im (CFIm) complex, which is essential for mRNA 3′ end processing [15]. They contribute to CFIm complex assembly by forming CPSF6 homodimers, CPSF7 homodimers, or CPSF6/CPSF7 heterodimers. Although *CPSF6* is established as the most frequent fusion partner for *RARG*, no rearrangements involving *CPSF6* with *RARA* or *RARB* have been reported to date. This patient represents the first reported case of a fusion between *CPSF7* and *RAR* gene.

The CPSF7 moiety within the fusion protein mirrors CPSF6 by retaining the N-terminal RNA recognition motif (RRM) while lacking the C-terminal arginine/serine-like domain (RSLD). The RRM module is required for RNA binding, CFIm complex assembly, and mRNA looping, whereas the RSLD of CPSF6 is essential for alternative polyadenylation and assembly of the mRNA 3′ end processing machinery [15]. Structurally, the tripartite fusion protein might be erroneously recruited to RNA processing hubs via the truncated CPSF7 component or, conversely, mislocalize CFIm factors to DNA promoter regions through the RARG DNA-

binding domain. This resulting “transcriptional and processing traffic jam” could interfere with the 3′ UTR length regulation of target genes, potentially driving aAPL pathogenesis—a hypothesis warranting further investigation.

Consistent with all previously identified tripartite *RARG* fusions, the 3′ splicing of *RARG* led to the loss of exon 10 and the encoded LBD-H11_12, providing the molecular basis for ATRA resistance. Consequently, all patients carrying *RARG* fusions exhibit primary resistance to ATRA therapy, as demonstrated by the case reported in this study. Our dual-luciferase reporter assays confirmed that, while a simulated bipartite *CPSF7*::*RARG* fusion retained ATRA sensitivity, the patient-specific tripartite *CPSF7*::*RARG*::*CPSF7* fusion was almost entirely non-responsive.

The leukemic cells in this case exhibited morphology and immunophenotype largely consistent with classical APL, except for CD38 negativity. This finding further supports that CD38 is consistently absent in *RARG* rearrangement cases, distinguishing this ATRA-resistant subtype from classical APL [6].

This patient harbored a somatic *ARID2* mutation. Given that *ARID2* is a fundamental component of the SWI/SNF complex required for nuclear receptor-mediated transcriptional activation, its disruption—alongside the loss-of-function *ARID1A*/*B* mutations previously reported by our group [3,7]—underscores that chromatin-remodeling dysregulation is likely a recurrently involved pathway in the pathogenesis of aAPL.

Clinical management was challenging due to the patient’s primary resistance to ATRA and multiple chemotherapeutic agents. CR was ultimately achieved through a combination of HHT, chidamide, selinexor, and an anti-CD33 monoclonal antibody. Selinexor was administered off-label under compassionate use, while chidamide was included based on prior in vitro evidence suggesting that HDAC3i could rescue dysregulated hematopoiesis in bipartite *CPSF6*::*RARG* fusions [8], despite its unclear efficacy in tripartite configurations.

Our functional analyses demonstrated that chidamide failed to restore transcriptional activity of the tripartite *CPSF7*::*RARG*::*CPSF7* fusion, while enhancing ATRA responsiveness in the bipartite *CPSF7*::*RARG* fusion (Figure 3C). Consequently, patients harboring tripartite *RARG*

fusions, characterized by LBD-H11_12 deletion, are unlikely to benefit from HDAC3i-based therapy.

In a collaborative study of *RARG*-aAPL clinical management, seven of eight patients achieved CR using HHT-based regimens, underscoring the therapeutic potential of HHT [6]. Consistently, recent in vitro studies have demonstrated the efficacy of HHT in mitigating *CPSF6*::*RARG*-driven dysregulated hematopoiesis [9]. While GO, an anti-CD33 antibody-drug conjugate, is increasingly utilized in high-risk *PML*::*RARA*-APL as a substitute for conventional chemotherapy [2], its application in aAPL has not been reported. In the present case, CR was achieved with a quadruple regimen comprising HHT, GO, chidamide, and selinexor after failure of multiple prior therapies. Given the complexity of this regimen, the individual contributions of each agent cannot be delineated, and further investigation is warranted.

In summary, we characterized the first case of aAPL harboring a tripartite *CPSF7*::*RARG*::*CPSF7* fusion. This case expands the repertoire of *RAR* fusion partners and reinforces the recurrence and structural consistency of tripartite *RARG* fusions via a novel 3′ splicing mode. Despite multi-drug resistance, the patient achieved CR through combined targeted and salvage therapy, followed by successful allo-HSCT. The rapid diagnosis and effective management of *RARG*-aAPL remain formidable challenges that necessitate continued exploration of its unique molecular landscape.

References

1. Rérolle D, Wu HC, de Thé H. Acute promyelocytic leukemia, retinoic acid, and arsenic: a tale of dualities. Cold Spring Harb Perspect Med. 2024;14(9):a041582.
2. Benitez LL, Marx KR, Rausch CR, et al. Multicenter retrospective evaluation of treatment for high-risk acute promyelocytic leukemia: real-world outcomes from the HERO Consortium. Am J Hematol. 2025;100(6):1094-1097.
3. Zhou X, Chen J, Tang YL, et al. Epidemiology, clinical features, and molecular basis of TTMV::RARA-driven acute promyelocytic leukemia. Blood. 2025;146(18):2229-2243.
4. Chen X, Wang F, Zhou X, et al. Torque teno mini virus driven childhood acute promyelocytic leukemia: the third case report and sequence analysis. Front Oncol. 2022;12:1074913.
5. Zhou X, Chen X, Chen J, et al. Critical role of tripartite fusion and LBD truncation in certain RARA- and all RARG-related atypical APL. Blood. 2024;114(14):1471-1485.
6. Zhu HH, Qin YZ, Zhang ZL, et al. A global study for acute myeloid leukemia with RARG rearrangement. Blood Adv. 2023;7(13):2972-2982.
7. Zhou X, Mu Q, Chen H, et al. Torque teno virus drives atypical acute promyelocytic leukemia as a novel molecular subtype. Am J Hematol. 2026;101(5):1084-1090.
8. Liu T, Wang T, Qi L, et al. CPSF6-RARγ interacts with histone deacetylase 3 to promote myeloid transformation in RARG-fusion acute myeloid leukemia. Nat Commun. 2025;16(1):616.
9. Wang F, Zhao L, Tan Y, et al. Oncogenic role of RARG rearrangements in acute myeloid leukemia resembling acute promyelocytic leukemia. Nat Commun. 2025;16(1):617.
10. Liu T, Wen L, Yuan H, et al. Identification of novel recurrent CPSF6-RARG fusions in acute myeloid leukemia resembling acute promyelocytic leukemia. Blood. 2018;131(16):1870-1873.
11. Han X, Jin C, Zheng G, et al. Acute myeloid leukemia with CPSF6-RARG fusion resembling acute promyelocytic leukemia with extramedullary infiltration. Ther Adv Hematol. 2021;12:2040620720976984.
12. Zhang Z, Jiang M, Borthakur G, et al. Acute myeloid leukemia with a novel CPSF6-RARG

variant is sensitive to homoharringtonine and cytarabine chemotherapy. Am J Hematol. 2020;95(2):E48-E51.

13. Wu S, Yu Y, Lin X, et al. Atypical acute promyelocytic leukemia with tripartite fusion gene PML::RARG::LINE-L2a is resistant to ATRA but sensitive to arsenic-based therapy. Haematologica. 2025;110(12):3083-3087.
14. Chen X, Yuan L, Zhang Y, et al. Advances towards genome-based acute myeloid leukemia classification: A comparative analysis of WHO-HAEM4R, WHO-HAEM5, and International Consensus Classification. Am J Hematol. 2024;99(5):824-835.
15. Liu S, Wu R, Chen L, et al. CPSF6 regulates alternative polyadenylation and proliferation of cancer cells through phase separation. Cell Rep. 2023;42(10):113197.

Figure legends

FIGURE 1. Morphological findings of the patient. (A) Wright staining of the peripheral blood smear at diagnosis showing aberrant promyelocytes with coarse azurophilic granules (×1000). (B) MPO staining of the peripheral blood smear demonstrating strong positivity in abnormal promyelocytes (×1000). (C) Timeline of the clinical course and treatment response of the patient. ATRA, all-trans retinoid acid; AZA, azacitidine; GO, gemtuzumab ozogamicin; HHT, homoharringtonine; HU, hydroxyurea; IAV, idarubicin/cytarabine/venetoclax; VEN, venetoclax.

FIGURE 2. Molecular identification of the patient. (A) UMAP clustering of gene expression profiles. The patient's transcriptomic profile clustered closely with canonical *PML*::*RARA* fusion-positive APL, while significantly distinct from other AML subtypes and healthy controls. (B) IGV view of the *ARID2* NM_152641.4:c.3563G>A/p.S1188N mutation detected in WTS. (C) Structural schematic of *CPSF7* exon 7::*RARG* exon 4 (top panel) and *RARG* exon 9::*CPSF7* exon 10@c.*1143 splicing (bottom panel) as analyzed by Arriba v2.5.1 software. AML, acute myeloid leukemia; APL, acute promyelocytic leukemia.

FIGURE 3. Fusion protein and cellular assay analysis. (A) Analysis of derived mRNA splice sites and fusion transcripts formed between *RARG* and the 3′ UTR of *CPSF7*. (B) Schematic diagram of *CPSF6*, *CPSF7*, *RARG*, and fusion transcripts. Red arrows indicate the breakpoints and splicing junctions at the genomic level during fusion transcripts formation. (C) Assessment of ATRA responsiveness was performed using a modified GAL4-UAS luciferase reporter assay in 293T cells. Constructs encoding the bipartite CPSF7::RARG (with intact LBD), the tripartite CPSF7::RARG::CPSF7, and the CPSF7::RARG-H11_12del mutant were cloned into the pBIND vector containing *Renilla* luciferase. CPSF7::RARG exhibited dose-dependent responsiveness to ATRA, similar to wild-type RARG (positive control). In contrast, the tripartite fusion and the H11_12del mutant showed no response. Chidamide significantly enhanced ATRA sensitivity in the bipartite CPSF7::RARG model (similar to its synergistic effect on wild-type RARG) but failed to rescue transcriptional activity in the tripartite fusion and the H11_12del mutant. Data are mean ± SD of three biological replicates. Welch's t-test was used for pairwise comparisons between groups (**P < 0.01, ***P < 0.001, ****P < 0.0001).

A representative experiment out of 3 with similar results is displayed. ATRA, all-trans retinoid acid; DBD, DNA binding domain; LBD, ligand binding domain; RRM, RNA recognition motif; RSLD, arginine/serine-like domain; UTR, untranslated region.

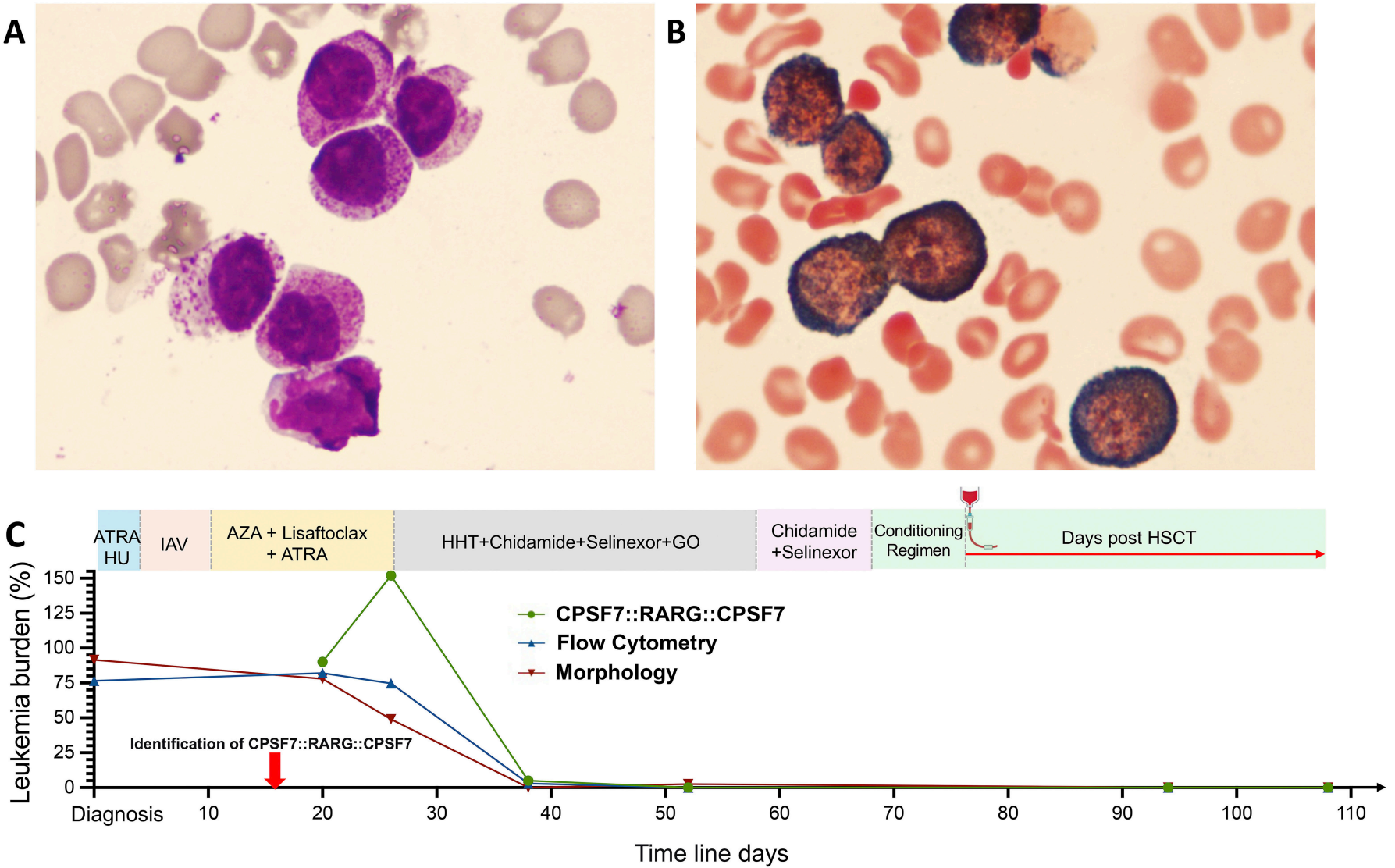
A
B
C
ATRA
HU
IAV
AZA + Lisaftoclax
+ ATRA
HHT+Chidamide+Selinexor+GO
Chidamide
+Selinexor
Conditioning
Regimen
Days post HSCT
CPSF7::RARG::CPSF7
Flow Cytometry
Morphology
Identification of CPSF7::RARG::CPSF7
Leukemia burden (%)
150
125
100
75
50
25
0
Diagnosis
10
20
30
40
50
60
70
80
90
100
110
Time line days

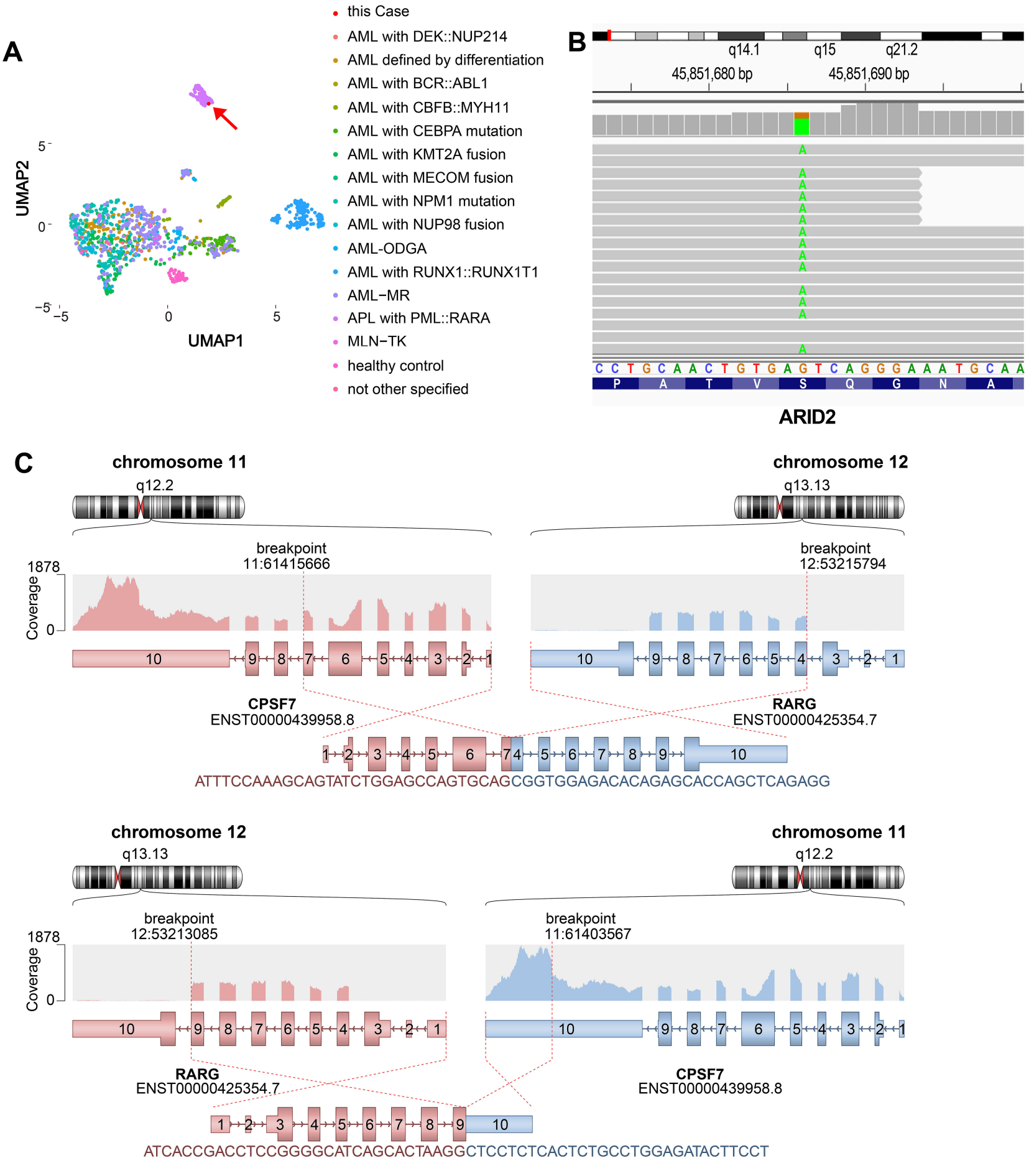
A
UMAP2
UMAP1
this Case
AML with DEK::NUP214
AML defined by differentiation
AML with BCR::ABL1
AML with CBFB::MYH11
AML with CEBPA mutation
AML with KMT2A fusion
AML with MECOM fusion
AML with NPM1 mutation
AML with NUP98 fusion
AML-ODGA
AML with RUNX1::RUNX1T1
AML−MR
APL with PML::RARA
MLN−TK
healthy control
not other specified
B
q14.1
q15
q21.2
45,851,680 bp
45,851,690 bp
C C T G C A A C T G T G A G T C A G G G A A A T G C A A
P A T V S Q G N A
ARID2
C
chromosome 11
q12.2
chromosome 12
q13.13
breakpoint
11:61415666
breakpoint
12:53215794
Coverage
1878
0
CPSF7
ENST00000439958.8
RARG
ENST00000425354.7
ATTTCCAAAGCAGTATCTGGAGCCAGTGCAGCGGTGGAGACACAGAGCACCAGCTCAGAGG
chromosome 12
q13.13
chromosome 11
q12.2
breakpoint
12:53213085
breakpoint
11:61403567
RARG
ENST00000425354.7
CPSF7
ENST00000439958.8
ATCACCGACCTCCGGGGCATCAGCACTAAGGCTCCTCTCACTCTGCCTGGAGATACTTCCT

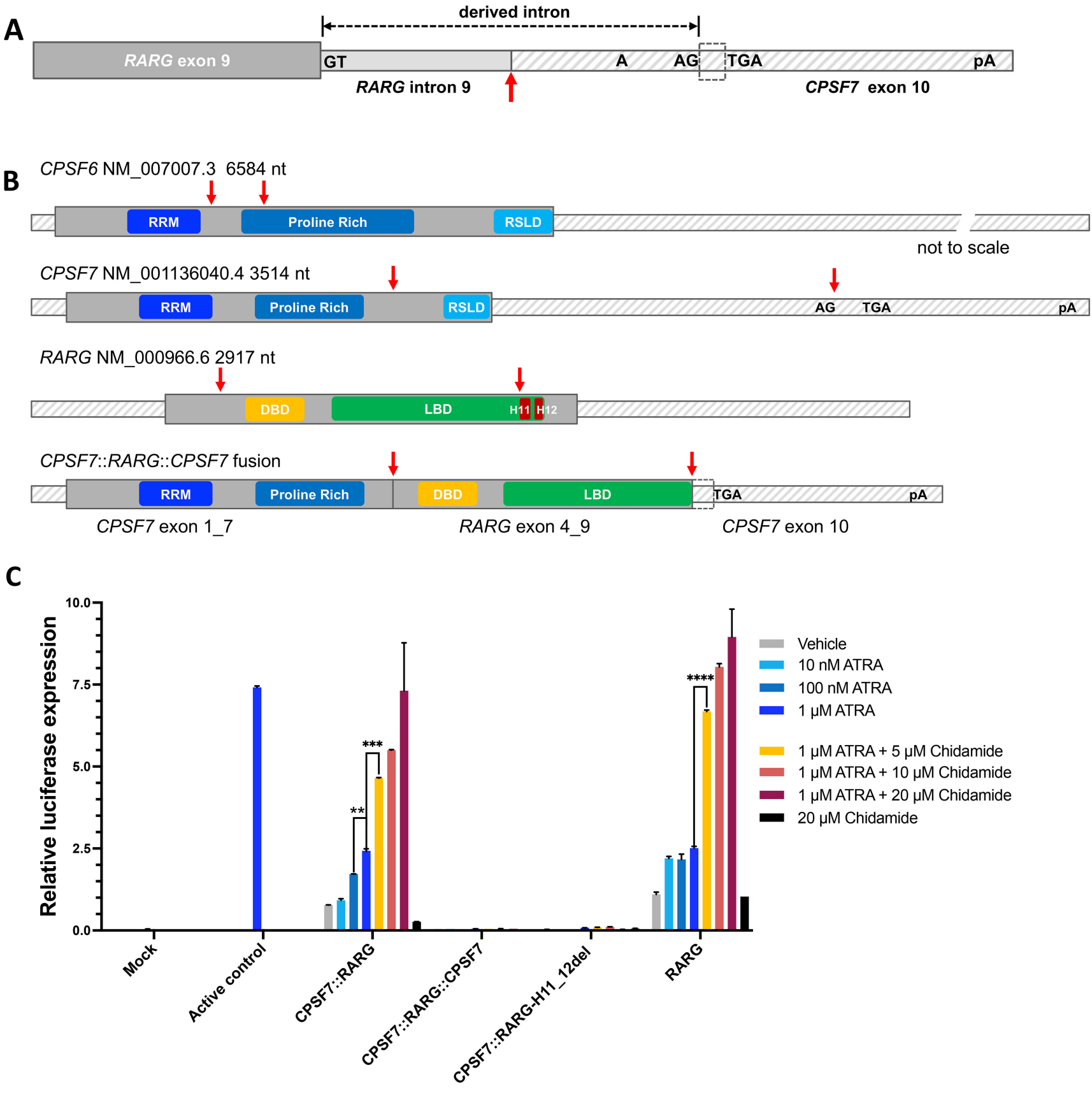
A
derived intron
RARG exon 9
GT
A
AG
TGA
pA
RARG intron 9
CPSF7 exon 10
B
CPSF6 NM_007007.3 6584 nt
RRM
Proline Rich
RSLD
not to scale
CPSF7 NM_001136040.4 3514 nt
RRM
Proline Rich
RSLD
AG
TGA
pA
RARG NM_000966.6 2917 nt
DBD
LBD
H11
H12
CPSF7::RARG::CPSF7 fusion
RRM
Proline Rich
DBD
LBD
TGA
pA
CPSF7 exon 1_7
RARG exon 4_9
CPSF7 exon 10
C
Relative luciferase expression
10.0
7.5
5.0
2.5
0.0
**
***
****
Vehicle
10 nM ATRA
100 nM ATRA
1 μM ATRA
1 μM ATRA + 5 μM Chidamide
1 μM ATRA + 10 μM Chidamide
1 μM ATRA + 20 μM Chidamide
20 μM Chidamide
Mock
Active control
CPSF7::RARG
CPSF7::RARG::CPSF7
CPSF7::RARG-H11_12del
RARG

Supplementary Table S1. 36 fusion genes included in our screening panel [1].

1.BCR-ABL1	2.BCR-FGFR1	3.CBFB-MYH11	4.DEK-NUP214
5.ETV6-ABL1	6.ETV6-PDGFRB	7.ETV6-RUNX1	8.FIP1L1-PDGFRA
9.FUS-ERG	10.KMT2A-AFF1	11.KMT2A-ELL	12.KMT2A-EPS15
13.KMT2A-MLLT1	14.KMT2A-MLLT3	15.KMT2A-MLLT4	16.KMT2A-MLLT6
17.KMT2A-MLLT7	18.KMT2A-MLLT10	19.KMT2A-MLLT11	20.KMT2A-PTD
21.NPM1-ALK	22.NPM1-MLF1	23.NPM1-RARA	24.NUP98-HOXA9
25.NUP98-HOXD13	26.PML-RARA	27.RPN1-MECOM	28.RUNX1-EAP
29.RUNX1-RUNX1T1	30.RUNX1-MECOM	31.SET-NUP214	32.STIL-TAL1
33.TCF3-HLF	34.TCF3-PBX1	35.ZBTB16-RARA	36.ZMYM2-FGFR1

[1] Chen, X., Wang, F., Zhang, et al. Panoramic view of common fusion genes in a large cohort of Chinese de novo acute myeloid leukemia patients. Leukemia & lymphoma. 2019;60(4):1071–1078.

Supplementary Figure S1

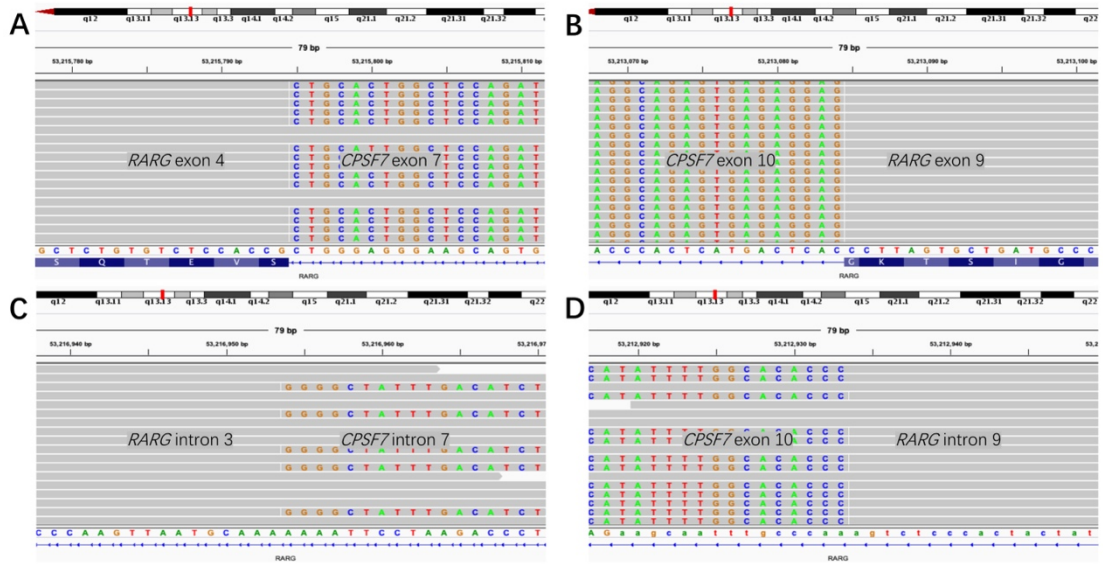

Supplementary Figure S1. IGV validation of the tripartite *CPSF7*::*RARG*::*CPSF7* fusion breakpoints. **A** IGV view of the *CPSF7* exon 7::*RARG* exon 4 splicing detected in WTS. **B** IGV view of the *RARG* exon 9::*CPSF7* exon 10@c.*1143 splicing detected in WTS. **C** IGV view of the *CPSF7* intron 7::*RARG* intron 3 splicing detected in WGS; **D** IGV view of the *RARG* intron 9 and *CPSF7* exon 10 splicing detected in WGS.

IGV, integrative genomics viewer; UMAP, Uniform Manifold Approximation and Projection; WGS, whole-genome sequencing; WTS, whole-transcriptome sequencing.